

Active diffusion of motor particles

Stefan Klumpp and Reinhard Lipowsky

Max-Planck-Institut für Kolloid- und Grenzflächenforschung, 14424 Potsdam-Golm, Germany

(Dated: January 1, 2018)

The movement of motor particles consisting of one or several molecular motors bound to a cargo particle is studied theoretically. The particles move on patterns of immobilized filaments. Several patterns are described for which the motor particles undergo non-directed but enhanced diffusion. Depending on the walking distance of the particles and the mesh size of the patterns, the active diffusion coefficient exhibits three different regimes. For micrometer-sized motor particles in water, e.g., this diffusion coefficient can be enhanced by two orders of magnitude.

PACS numbers: 87.16.Nn, 81.07.-b, 05.40.-a

Introduction. Biological motor molecules such as the cytoskeletal motors kinesin and myosin, which convert the chemical free energy released from the hydrolysis of adenosine triphosphate (ATP) into directed movements along cytoskeletal filaments, represent powerful nanomachines. It seems rather promising to construct artificial biomimetic devices based on these molecular motors and to use them, e.g., for the transport of cargo particles in the nano- and micrometer regime [1, 2]. These approaches are based on two different *in vitro* motility assays, the gliding assay, for which molecular motors are anchored at a substrate surface and drag filaments along this surface, and the bead assay, for which the filaments are immobilized on the surface and the motors pull beads or cargo along these filaments [3].

In order to obtain *spatial control* of the movements, motor molecules or filaments can be bound to the substrate surface in well defined patterns by controlling the surface topography and/or chemistry. Examples are motor-covered surface channels or grooves which guide the gliding filaments, chemical patterning of a surface to bind filaments or motors selectively, and combinations of topographic and chemical patterning, see, e.g., [4, 5, 6, 7, 8, 9, 10]. In this way, one can create 'active stripes' along which the active transport takes place. The *directionality* of these stripes can be controlled in a rather direct way for systems based on the bead assay, since unidirectional movement of motors can be realized by aligning filaments in parallel with the same orientation [9, 10]. In gliding assays, movement of filaments usually occurs randomly in both directions, but unidirectional movements can be obtained constructing special surface domain patterns [7].

Usually, molecular motors undergo *directed movements* which can be used for transport over large distances. However, the active motion of molecular motors can also be used to generate *effectively diffusive movements* by sequences of active directed movements into random directions. We will call these ATP-dependent and thus energy-consuming, but effectively non-directed movements *active diffusion*. It should be useful under conditions where simple diffusion is slow, i.e., for large car-

goes or high viscosity of the fluid. Active diffusion is also present *in vivo*, where various motor-driven cargoes such as vesicles, messenger RNA, and viruses exhibit active back-and-forth movements [11].

In the following, we will discuss active diffusion in several simple systems which can be realized experimentally. We present results for several cases where patterns of 'active stripes' have been created on a surface by immobilizing cytoskeletal filaments in certain well-defined patterns, so that they constitute a system of tracks for the active movements of particles coated with molecular motors. Even though we focus on these latter systems derived from bead assays with mobile motors, our arguments can be easily extended to mobile filaments gliding in motor-covered surface grooves.

Model. In order to study the effective diffusion arising from active motion along patterns of filaments, we describe these movements as random walks on a lattice [12, 13]. We consider a cubic lattice with lattice constant ℓ on which certain lines of lattice sites represent the filaments or active stripes. If a motor-driven particle occupies such a lattice site, it makes a forward step (along the orientation of the filament), a backward step, and no step with probabilities α , β , and γ per time unit τ , respectively. In addition, it may escape to each of the n_{ad} adjacent non-filament sites with probability $\epsilon/6$ ($n_{\text{ad}} = 3$ and 4 for a filament at a wall and in solution, respectively). An unbound particle, i.e., a particle at

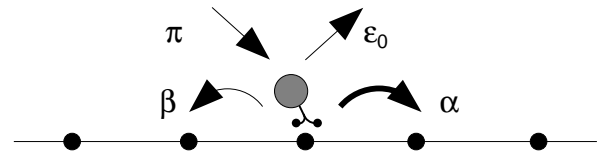


FIG. 1: Lattice model for the active motor movements along filaments. Motors make forward and backward steps along the filament with probabilities α and β , respectively and no step with probability γ . Unbinding from the filament occurs with probability $\epsilon_0 = n_{\text{ad}}\epsilon/6$ where n_{ad} is the number of non-filament neighbor sites, and a motor reaching the filament binds to it with sticking probability π_{ad} .

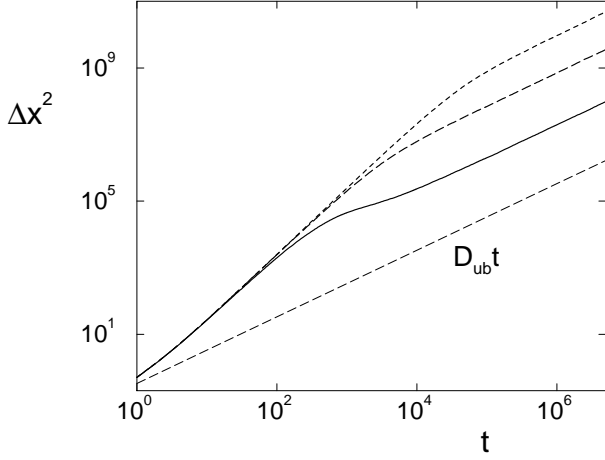


FIG. 2: Active diffusion in a tube with two antiparallel filaments (double-logarithmic plot): The variance Δx^2 of the particle position as a function of time t for motor-driven particles with unbinding probabilities $\epsilon = 0.01$ (solid), 10^{-3} (dashed), and 10^{-4} (dotted line) and other parameters as described in the text. The thin dashed line indicates unbound diffusion which is much smaller than active diffusion. Here and in the following figures, lengths and times are expressed in units of ℓ and τ , respectively.

a non-filament site, performs a symmetric random walk and steps to each neighbor site with probability $1/6$ per time τ . An unbound motor reaching a filament site binds to it with probability π_{ad} . The parameters of the random walks can be adapted to the measured transport properties [12]. Confining surfaces are implemented by rejecting all stepping attempts to lattice sites of the surfaces.

For the simulations, we chose the basic length scale to be $\ell = 50\text{nm}$ and the basic time scale to be $\tau = 25\text{ms}$. These values result in a diffusion coefficient $D_{\text{ub}} \sim 10^{-1}\mu\text{m/s}$ as appropriate for a micrometer-sized particle in water. We take $\alpha = 0.5$, $\beta = 0$, and $\pi_{\text{ad}} = 1$, corresponding to a velocity $v_b \simeq 1\mu\text{m/s}$ and a binding rate in the order of 100s^{-1} for motors within a capture range of 50nm from the filament.

Active diffusion in 1d. In order to discuss the simplest case of active diffusion, let us consider two parallel filaments with opposite polarity. We denote the coordinate axis parallel to the filaments by x and take the filaments to be sufficiently long, so that the filament ends are not reached within the observation time. The filaments are placed within a long and thin tube or channel with a rectangular cross section (with width L and height H), so that unbound motors cannot escape, but rebound with a finite mean return time, a situation that mimics the axon of a nerve cell.

We have studied this case using an analytical Fourier–Laplace technique as in Refs. [13] and computer simulations. Some results are shown in Fig. 2. Because of the antiparallel orientation of the filaments, no net movement

is obtained in such a system, and the effective velocity is zero on large scales. The effective diffusion coefficient, $D \equiv \lim_{t \rightarrow \infty} \Delta x^2(t)/2t$, defined via the long-time behaviour of the positional variance $\Delta x^2 \equiv \langle x^2 \rangle - \langle x \rangle^2$, is found to be given by

$$D = \bar{D} + D_{\text{act}}P_b, \quad (1)$$

where the first term is the weighted average of the bound and unbound diffusion coefficient, $\bar{D} = D_b P_b + D_{\text{ub}}(1 - P_b)$ with the probability $P_b = 1/[1 + (\epsilon/\pi_{\text{ad}})LH/\ell^2]$ that the motor is bound to the filament at large times. The contribution of the bound diffusion coefficient is usually small, so that $\bar{D} \simeq D_{\text{ub}}(1 - P_b)$. The second term describes active diffusion, i.e., additional spreading of a distribution of many motors due to the active directed movements into both directions with

$$D_{\text{act}} = \frac{3v_b^2}{2\epsilon}. \quad (2)$$

The latter contribution can be written as $D_{\text{act}} = \frac{1}{2}\langle L_s^2 \rangle / \Delta t_b = \Delta x_b v_b$ with the average walking time $\Delta t_b = 3/(2\epsilon)$, the average walking distance $\Delta x_b = v_b \Delta t_b$, and the mean square of the distance L_s traveled actively before a change of direction via unbinding, as obtained from the distribution $P(L_s) = \frac{1}{2\Delta x_b} e^{-|L_s|/\Delta x_b}$ of the walking distances.

This contribution is present even if the diffusive motion of unbound motors is strongly suppressed, e.g. because of their large cargoes or because of a high viscosity of the fluid. In cells, this should apply to the movements of large organelles such as mitochondria (where, however, the switching of direction is accomplished via different types of motors rather than via the orientation of the filaments) [11].

Active diffusion as given by $\Delta x^2 \approx 2Dt$ is valid at large times with $t \gg t_* \equiv 2D/v_b^2 \simeq 3P_b/\epsilon$, see Fig. 2. Note that the larger the active diffusion coefficient, the larger is also the crossover time t_* and, thus, the time necessary to observe the active diffusion.

An enhancement of diffusion occurs also in rather different contexts such as electrophoresis, chromatographic columns, and diffusion in hydrodynamic flow which can also be described by multi-state random walk models [14, 15]. In all of these cases, however, the directed motion arises from externally applied fields rather than from the active movements of the motor particles.

Arrays of filaments on a surface. Let us now consider filaments which are immobilized on patterned surfaces with two-dimensional arrays of stripes. We consider four systems as shown in Fig. 3: (A1, A2) consist of arrays of parallel stripes whereas (B1, B2) correspond to intersecting stripes which form a two-dimensional square lattice with lattice constant L . The stripes have a width W ; in our simulations, we used $W = \ell$. In both cases, we studied two situations: (i) Each stripe contains filaments with both possible orientations as in (A1, B1),

and motor particles which bind to a stripe can start to move in either direction (which is chosen randomly in the simulations); and (ii) neighboring stripes are covered by filaments with opposite orientation as in (A2, B2). Note that all patterns have no directional bias on large scales.

The motors can change their direction of movement via unbinding and rebinding to another filament. In the stripe lattices, they can also change direction at the vertices by switching to another filament, which is chosen randomly. Finally, we take the diffusion in the direction perpendicular to the surface to be restricted to a slab of height H . To study the active diffusion for this case, we determined the diffusion coefficient by extensive Monte Carlo simulations for motor-driven active particles of micrometer size and for a wide range of the unbinding rate ϵ and the stripe separation L as shown in Fig. 4.

Arrangements of filaments of this type are accessible to experiments and can be created using structured surfaces as described above. Lattice patterns of filaments can also be formed by the self-organization of filaments and motor complexes [16] or by the assembly of crosslinked networks on micropillars [17].

Parallel active stripes. Arrays of parallel active stripes which contain filaments with both orientations (A1) exhibit active diffusion very similar to the one-dimensional case discussed above. However, in this case, the effective diffusion coefficient depends on the spatial direction. While the effective diffusion is described by Eq. (1) in the direction parallel to the stripes, which leads to the parallel diffusion coefficient $D_{\parallel} = \bar{D} + D_{\text{act}}P_b$, the diffusion perpendicular to the stripes is characterized by $D_{\perp} = D_{\text{ub}}(1 - P_b)$, see Fig. 4(a). The latter expression is also valid if the directionality of the stripes alternates (A2), where the unbound motors return predominantly to the same stripe which leads to a higher value of D_{\parallel} as shown in Fig. 4(a).

Regular lattices of active stripes. In the system architectures (B1,B2), the motor-driven active particles can perform two-dimensional random walks on the stripe lattice even if they remain bound to the filaments. In addition, effectively diffusive behavior can arise from the repeated unbinding from and binding to filament. Let us consider case (B1). The diffusion coefficient is given by $D = D_{\text{act}}P_b + D_{\text{ub}}(1 - P_b)$ with $P_b \approx 1/[1 + (\epsilon/\pi_{\text{ad}})LH/(2W\ell)]$ for the stripe lattice. Depending on the processivity of the active particles, i.e. on the value of the unbinding rate, there are three regimes:

(I) If the unbinding rate is small, so that the walking distance is large compared to the pattern mesh size, $\Delta x_b = 2v_b/\epsilon \gg L$, the particle performs a random walk along the active stripe lattice and the diffusion coefficient is $D \approx D(\epsilon = 0) = \frac{1}{4}v_bL$. This case should be appropriate for cargo particles driven by many processive motors.

(II) If the average walking distance before unbinding is smaller than the mesh size, $\Delta x_b = 2v_b/\epsilon \ll L$ as appropriate, e.g., for transport by single processive motors,

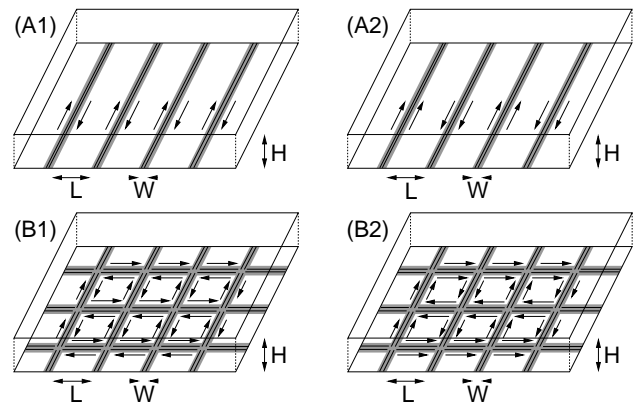


FIG. 3: Substrate surfaces with active stripes which consist of filaments immobilized onto striped surface domains: For the system architectures (A1) and (B1), all stripes contain filaments with both orientations, for (A2) and (B2), the filaments within one stripe have the same orientation, but filaments on neighboring stripes have opposite orientation.

changes in direction of movement will mainly be through unbinding and rebinding to another filament. In that case, the distance traveled before a change of direction is given by the walking distance Δx_b and, similar to the one-dimensional case discussed before, the diffusion coefficient is $D \approx \frac{1}{2}\Delta x_b v_b P_b$ [18].

(III) Finally, if motor particles spend most of the time unbound, i.e., for large ϵ as appropriate for weakly processive motors, the diffusion coefficient is simply given by the unbound Brownian motion, $D \approx D_{\text{ub}}$.

The three regimes can be summarized in one formula by using $D_{\text{act}} = v_b L_s/4$ and defining the interpolated distance traveled between two changes of direction by $L_s = L2\Delta x_b/(L + 2\Delta x_b)$ which leads to

$$D = \frac{v_b}{2} \frac{L\Delta x_b}{L + 2\Delta x_b} P_b + D_{\text{ub}}(1 - P_b). \quad (3)$$

The latter expression leads to the solid line in Fig. 4(b), which agrees well with the data points (open circles) from our simulations.

The value of the active diffusion coefficient can be further enhanced by controlling the orientation of the filaments along the stripes, i.e., by using filament patterns such as (B2) for which we obtain an active diffusion coefficient twice as large as for case (B1). In regime (I) this factor is due to the fact that a fully random choice of the new direction is completed after a walk over the distance $2L$. However, Eq. (3) with an additional factor of two in the active diffusion term describes rather well our simulation data also in regime (II).

Discussion. Finally, let us estimate the order of magnitude of the active diffusion in systems that are experimentally accessible. Free diffusion in a Newtonian fluid is governed by the Stokes–Einstein relation from which the diffusion coefficient is obtained as $D_{\text{ub}} \approx$

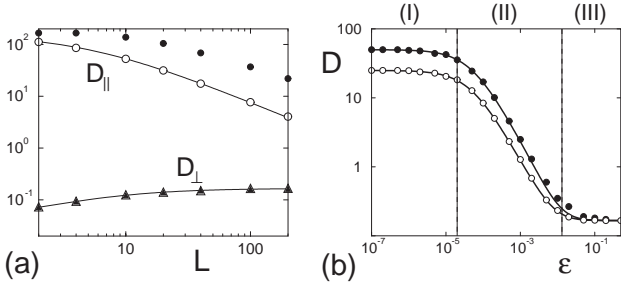


FIG. 4: (a) Effective diffusion coefficients D_{\parallel} (circles) and D_{\perp} (triangles) as functions of the stripe separation L . The open and filled symbols correspond to the two system architectures (A1) and (A2), respectively, compare Fig. 3. The full lines indicate the analytical result for (A1). (b) Effective diffusion coefficient D as a function of the unbinding probability ϵ . D exhibits three regimes (I)–(III) as discussed in the text. The open and filled symbols correspond to the two system architectures (B1) and (B2), respectively, as in Fig. 3. The parameters are as described in the text; we used $\epsilon = 0.0025$, $H = 100\ell$ in (a) and $L = H = 100\ell$ in (b).

$(100\text{nm}/R_{\text{hyd}}) \times 2.4\mu\text{m}^2/\text{s} \times \eta_{\text{water}}/\eta$. In the latter expression, R_{hyd} is the effective hydrodynamic radius of the particle and η the viscosity of the medium. For a micrometer-sized particle in water, we have $D_{\text{ub}} \sim 0.1\mu\text{m}^2/\text{s}$, for a 100nm-sized particle $D_{\text{ub}} \sim 1\mu\text{m}^2/\text{s}$. (The diffusion coefficient of bound motors moving along filaments is much smaller, typically of the order of $D_{\text{b}} \sim v_{\text{b}}\ell \sim 0.01\mu\text{m}^2/\text{s}$ with $v_{\text{b}} \sim 1\mu\text{m}/\text{s}$ and $\ell \sim 10\text{nm}$.)

The active diffusion coefficient, on the other hand, is of the order of $\frac{1}{4}v_{\text{b}}L_sP_{\text{b}}$ with L_s given by the filament length in regime (I) and by the walking distance in regime (II). With a typical filament length of a few tens of μm , this means that active diffusion coefficients of the order of $10\mu\text{m}^2/\text{s}$ can be obtained for cargo particles driven by many motors, for which regime (I) is appropriate. For micrometer-sized particles this is two orders of magnitude larger than the diffusion coefficient of unbound Brownian motion. For cargo particles driven by a single or a few motors, regime (II) applies, and for a typical unbinding rate of $1/\text{s}$, we obtain an active diffusion coefficient of $\sim 1\mu\text{m}^2/\text{s}$.

These estimates as well as our simulation data are for diffusion in water. In a more viscous medium with viscosity $\eta > \eta_{\text{water}}$, diffusion is even more enhanced due to the active processes, because active diffusion does not obey the Einstein relation and is largely independent of η [19]: the viscous force on a micrometer-sized bead moving with $1\mu\text{m}/\text{s}$ is of the order of $\sim \eta/\eta_{\text{water}} \times 10^{-2}\text{pN}$ which is small compared to the piconewton forces required to slow down the active movements of a single motor. Unbound diffusion is however reduced by the factor η_{water}/η , so that the ratio $D/D_{\text{ub}} \sim \eta$ increases with increasing viscosity η .

Active diffusion will therefore be useful for particles

which explore surface patterns with linear dimensions of tens of micrometers or even millimeters, e.g., in order to find a specific binding partner or to deliver a cargo, in particular if the surrounding fluid has a high viscosity. One potential application is provided by the integration of these biomimetic transport systems into labs-on-a-chip for genomics or proteomics.

In summary, we propose here to use chemically or topographically patterned surfaces to create well defined arrangements of active stripes covered by filaments and to use the random walks arising from the active movements of motor-covered particles along these stripes to achieve fast diffusion on the surface.

-
- [1] H. Hess and V. Vogel, *Rev. Mol. Biotechnology* **82**, 67 (2001).
 - [2] K. J. Böhm and E. Unger, in *Encyclopedia of Nanoscience and Nanotechnology*, edited by H. S. Nalwa (American Scientific Publishers, Stevenson Ranch, 2004), vol. 4, pp. 345–357.
 - [3] J. Howard, *Mechanics of Motor Proteins and the Cytoskeleton* (Sinauer Associates, Sunderland, 2001).
 - [4] H. Suzuki, A. Yamada, K. Oiwa, H. Nakayama, and S. Mashiko, *Biophys. J.* **72**, 1997 (1997).
 - [5] D. Riveline, A. Ott, F. Jülicher, D. A. Winkelmann, O. Cardoso, J.-J. Lacapère, S. Magnúsdóttir, J.-L. Viovy, L. Gorre-Talini, and J. Prost, *Eur. Biophys. J.* **27**, 403 (1998).
 - [6] H. Hess, J. Clemmens, D. Qin, J. Howard, and V. Vogel, *Nano Lett.* **1**, 235 (2001).
 - [7] Y. Hiratsuka, T. Tada, K. Oiwa, T. Kanayama, and T. Q. P. Uyeda, *Biophys. J.* **81**, 1555 (2001).
 - [8] D. C. Turner, C. Chang, K. Fang, S. L. Brandow, and D. B. Murphy, *Biophys. J.* **69**, 2782 (1995).
 - [9] K. J. Böhm, R. Stracke, P. Mühlig, and E. Unger, *Nanotechnology* **12**, 238 (2001).
 - [10] L. Limberis, J. J. Magda, and R. J. Stewart, *Nano Lett.* **1**, 277 (2001).
 - [11] S. P. Gross, *Phys. Biol.* **1**, R1 (2004).
 - [12] R. Lipowsky, S. Klumpp, and T. M. Nieuwenhuizen, *Phys. Rev. Lett.* **87**, 108101 (2001).
 - [13] T. M. Nieuwenhuizen, S. Klumpp, and R. Lipowsky, *Europhys. Lett.* **58**, 468 (2002) and *Phys. Rev. E* **69**, 061911 (2004).
 - [14] G. Weiss, *Aspects and Applications of the Random Walk* (North-Holland, Amsterdam, 1994).
 - [15] C. Van den Broeck, *Physica A* **168**, 677 (1990).
 - [16] T. Surrey, F. Nédélec, S. Leibler, and E. Karsenti, *Science* **292**, 1167 (2001).
 - [17] W. H. Roos, A. Roth, J. Konle, H. Presting, E. Sackmann, and J. P. Spatz, *ChemPhysChem* **4**, 872 (2003).
 - [18] The width of regime (II) can be increased by an increase of v_{b} which shifts regime (I) to smaller ϵ and by increasing π_{ad} which shifts regime (III) to larger ϵ .
 - [19] For a linear force-velocity relation, $v_{\text{b}} = v_{\text{b,max}}/[1 + 10^{-3} \times \eta/\eta_{\text{water}}(R_{\text{hyd}}/1\mu\text{m})/N]$, where N is the number of motors driving a cargo particle.